January 2012

Tissue-Engineered Vascular Grafts Allow Neovessel Formation By Recruiting Adjacent Vascular Tissue

Adam Shoffner

Tissue-engineered vascular grafts allow neovessel formation by recruiting adjacent vascular tissue

A Thesis Submitted to the
Yale University School of Medicine
In Partial Fulfillment of the Requirements for the
Degree of Doctor of Medicine

by
Adam Shoffner
2012

TISSUE-ENGINEERED VASCULAR GRAFTS ALLOW NEOVESSEL FORMATION BY RECRUITING ADJACENT VASCULAR TISSUE.

Adam Shoffner, Narutoshi Hibino, Gustavo Villalona, Nicholas Pietris, Daniel R. Duncan, Jason D. Roh, Tai Yi, Lawrence W. Dobrucki, Dane Mejias, Rajendra Sawh-Martinez, Jamie K. Harrington, Albert Sinusas, Diane S. Krause, Themis Kyriakides, W. Mark Saltzman, Jordan S. Pober, Toshiharu Shin'oka, and Christopher K. Breuer.

Interdepartmental Program in Vascular Biology and Therapeutics, Yale University, School of Medicine, New Haven, Connecticut, USA.

Hypothesis: Tissue Engineered Vascular Grafts (TEVGs) constructed by seeding cells autologous bone marrow-derived mononuclear cells onto dissolvable scaffolding aid in the recruitment of cells from either the host's bone marrow or neighboring vasculature to form the graft neotissue.

Methods: RT-PCR was performed on explanted grafts to detect presence of seeded cells. FISH for Y chromosome was performed on female mice with male bone marrow transplant along with female mice with implanted male-composite TEVG.

Results: The seeded cells on implanted TEVGs decrease precipitously from 4.37% to 0.02% from 6hr to 14 days. At 6 months post implantation composite graft TEVGs displayed a high percentage of Y chromosome-positive cells adjacent to male inferior vena cava tissue. Explanted grafts from female mice following male bone marrow transplant revealed no neotissue positive for Y chromosome.

Discussion: TEVGs derive their neotissue from adjacent vasculature following implantation that is mechanistically aided by the presence of seeded bone marrow-derived mononuclear cells.

Acknowledgements:

I would like to thank Dr. Christopher Breuer for allowing me to work in his laboratory. Additionally Gustavo Villalona & Narutoshi Hibino for their help in designing experiments and their mice work that was absolutely critical for these experiments.

Table of Contents:

Introduction:

In North America, Congenital Heart Defects (CHDs) continue to be the leading cause of death within the infant population (1). Occurring in approximately 0.8% of live births some CHDs are clinically non-significant, however others are clearly associated with significant morbidity and mortality (2). Many less severe CHDs are readily controllable with observation and medical therapy. However, more complicated defects such as tetrology of Fallot and single ventricle defects require surgical methods for the establishment of physiologic blood flow (3).

The atria, ventricles, valves, and great vessels can all be anomalous in CHDs (4). Occasionally a primary repair of the defect is possible. However, often the use of a prosthetic graft is necessary for anatomical continuity in cases of greater complexity such as in single ventricle anomalies. These single ventricle anomalies include pulmonary or tricuspid atresia along with hypoplastic left heart syndromes (4). Together, these represent one of the largest groups of CHDs that can result in life-threatening disease as they allow for the mixing of oxygenated and deoxygenated blood and resultant chronic hypoxia and cyanosis. Additionally, the mixing of blood can cause volume overload leading to heart failure. Left untreated, mortality during the first year of life is 70% (5).

Since its introduction in 1971 the Fontan procedure (6) has been the treatment of choice for single ventricle anomalies. The ultimate goal of the

procedure is to separate the pulmonary from systemic circulation (7,8). This involves the diversion of blood into the pulmonary artery directly from the inferior vena cava (IVC) and is known as the modified Fontan operation with extra cardiac total cavopulmonary connection (EC TCPC) (7,8).

Traditionally the Fontan procedure has required a prosthetic vascular conduit to direct the blood from either the IVC or right atrium (6). Other CHDs requiring prosthesis include tetrology of Fallot and coarctation of the aorta. Tetrology of Fallot may require a vascular conduit to establish flow from the right heart to the pulmonary circuit in a similar manor to the Fontan procedure (4,9,10,11). Patients may also require a prosthetic valve to repair a diseased valve (12). Coarctation of the aorta may require a prosthetic vascular conduit connecting the aorta, distal to the coarctation, to the left ventricle. Additionally, large atrial or ventricular septal defects may require prosthetic patches for repair (4).

These procedures and the use of prosthetic grafts have led to rapid development and improvements in the field of pediatric cardiothoracic surgery over the last century. However, despite these improvements there continues to exist significant morbidity and mortality associated with the repair of CHDs (13,14). There are several reasons for this continuation. One reason being that advancements in the field have allowed surgeons to

attempt repairs of the most complex defects (4). A second reason is that the use of prostheses is not without their pitfalls. Synthetic vascular grafts currently in use, such as polytetrafluoroethylene, lack the ability to grow. Additionally they have numerous problems associated with the development of thrombosis, ectopic calcification, and increased infection susceptibility (15,16). These problems with synthetic prostheses have contributed to the continued morbidity and mortality associated with the repair of CHDs. The lack of prosthesis growth potential often forces the pediatric patient to endure multiple procedures to upsize the graft as the patient grows. This exposes the patient to the morbidity and mortality associated with having to undergo multiple surgeries (14). Two strategies have been used in an effort to address the lack of growth potential. The first strategy is to delay surgery until the patient has reached a suitable size allowing for the implantation of an adult-sized graft (17). A second option is the implantation of an oversized graft. There are problems associated with both options. The delay of surgery can result in both volume overload and chronic hypoxia. Chronic hypoxia has been associated with developmental delays and failure to thrive (18). Volume overload may cause cardiac failure. The option to use an oversized graft often results in turbulent blood flow which increases the risk of thromboembolic complications which are a leading cause of graft failure and postoperative morbidity and mortality (17).

Due to these limitations associated with prosthetic grafts, alternatives that address these issues could greatly reduce the morbidity and mortality that is currently associated with surgical repair of CHDs. Tissue-engineered vascular grafts (TEVGs) have recently been shown to provide an attractive alternative to prosthetic grafts (19-22). A number of approaches, including in vivo blood vessel engineering, the use of explanted native vessels as a living scaffold, using biodegradable polymeric scaffolds onto which various cells can be seeded prior to implantation, and scaffold-free approaches have all been investigated (23-25). Unfortunately, none of these have resulted in the creation of an ideal TEVG.

TEVGs constructed from the seeding of a biodegradable polymeric scaffolding with cells has revealed promising results. Shinoka *et al.* described the first implantations of TEVGs into 25 pediatric patients for the repair of single ventricle defects in 2001 (26-28). The conduits were used to create EC TCPC during repair of right ventricle outflow defects or single ventricle anatomy (29,30). A poly-L-lactide (PLLA) with a copolymer of lactide and ε-caprolactone (P(CL/LA)) was seeded with autologous bone marrow mononuclear cells (BM-MNC) harvested on the day of the surgery. Prior to implantation, seeded conduits were maintained in culture media for 2-4 h (29). All of the patients that received a TEVG were evaluated by echocardiography, angiography, computerized tomography, and/or magnetic resonance imaging. Long-term follow-up has

revealed graft stenosis in 16% of patients, however this was typically asymptomatic and all have been treated successfully with stenting and angioplasty.

Based on these data the use of TEVGs as EC TCPC for the repair of single ventricle defects is very promising as it has been shown to be both safe and effective. However, despite these encouraging results, the mechanisms that underlie the process of graft formation and failure continue to remain poorly understood. It has been hypothesized that the formation of neotissue forms from cells that have been seeded onto the biodegradable scaffold (31). Within this hypothesis these seeded cells are believed to divide and differentiate into endothelial cells as the scaffold degrades, resulting ultimately in a purely biological structure without any synthetic components that has the ability to repair, remodel, and grow in concert with the patient.

In an effort to better understand these underlying processes we miniaturized the procedure to allow for a TEVG to be implanted as an IVC interposition graft in a mouse recipient. Scaffolds were created from the same synthetic materials and design as used clinically to allow for the retention of structural, mechanical, and degradation properties.

Statement:

It was hypothesized that, contrary to the accepted paradigm, autologous bone marrow-derived mononuclear cells (BMMCs) when seeded onto a biodegradable scaffold and implanted into mice as tissue engineered vascular grafts (TEVGs) that seeded cells do not differentiate and divide to become the neotissue. Furthermore it was hypothesized that the source of the cells that ultimate become neotissue was either the vasculature adjacent to the implanted TEVG or cells arising in the host's own bone marrow.

Methods:

In the following methods I performed the experiments involved with all qRT-PCR. This includes the isolation and purification of DNA from mice, the generation of a reproducible standard curve allowing for the measurement of mouse genomes/μL, design of the primers and probes, and the qRT-PCR performed on all explanted mouse TEVGs. All other experiments were performed by other members of the laboratory.

- *Isolation & purification of DNA from GFP + Mice*

With the ultimate goal of creating a quantitative Polymerase Chain Reaction (qPCR) experiment that would allow for the tracking of Green Fluorescent Protein (GFP)-positive mouse cells in explanted Tissue Engineered Vascular Grafts (TEVGs), purified whole mouse genomic DNA was initially needed from both GFP-positive and GFP-negative mice. This

DNA was needed for the creation of both positive and negative controls to test and optimize the primers necessary for the reaction. Additionally, the DNA was required for the creation of a DNA standard curve that would ultimately allow for the quantification of GFP-positive genomes in the explanted mouse samples. After concentrating the cells, approximately 5 x 10^6 GFP-positive Bone Marrow-Derived Mononuclear Cells (BM-MNCs obtained from C57BL/6 GFP-positive mice were resuspended in 200 uL lysis buffer (Qiagen, Valenica, CA, USA) and incubated overnight at 56° C in Proteinase K (12 mAu/reaction) to aid in the DNA extraction. Following tissue digestion, the whole genomic DNA was then isolated using DNeasy blood and tissue kit (Qiagen) following the manufacturer's instructions. DNA was eluted from the column with 200 uL Buffer AE (Qiagen) and stored at + 4° C. For use as a negative control in downstream experiments, DNA was isolated from (non-GFP + mice) in a manor identical to that previously described. The DNA concentrations were then determined using the NanoDrop ND-1000 (NanoDrop, Wilmington, DE, USA) per manufacture's instruction.

- *Standard Curve Generation*

The creation of the standard curve is one of the most important aspects of this experiment. The standard curve allows for the determination of the amount of DNA present in unknown samples. Using the molecular weight of the mouse genome at 4 x 10^{12} grams/mol (32) the DNA concentration with the units genomes/μL was determined. A working dilution of 20,000

genomes/μL was created. This allowed for 10-fold serial dilutions to be performed by placing 20 μL of DNA into 180 μL ddH_2O to a concentration of .2 genome/μL. These dilutions were subsequently used as qPCR standards by adding 5 μL of each concentration to each reaction resulting in a standard curve from $1x10^5$ genomes to 1 genome. The standard curve was run in triplicate in all experiments.

- *Design of primers & probe*

The gene of interest in this experiment is the GFP gene. Since its discovery in the 1960s (33) the GFP gene has been modified numerous times creating multiple different gene sequences. The most popular of these is the enhanced-GFP (EGFP) mutant (34) that allows for use of the gene in mammalian cells. In an effort to ensure that the primers designed for this experiment would be useful across numerous GFP strains the most common three GFP strains were compared. Using guidelines to ensure a G-C content of approximately 20-80%, avoidance of consecutive identical nucleotides, avoidance of a guanine on the 5' end, and an ideal melting temperature of 68° primers were designed that adhered to these rules and amplified a 93 base pair region that was completely conserved between the three GFP strains. (Applied Biosystems) The following primers and probe were chosen: forward, 5' –ACCACATGAAGCAGCACGACTTCT- 3'; reverse, 5' –TGTAGTTGCCGTCGTCCTTGAAGA- 3'; probe, 5'-AAGGCTACGTCCAGGAGCGCACCAT- 3'. The primers were synthesized by W.M. Keck Oligonucleotide Synthesis Facility at Yale University. The

primers were reconstituted in H_2O, the amount of which was determined by multiplying the total nanomoles of primer by four with the product being the volume of H_2O added. Theoretically this should yield a final primer concentration of 250 uM. The concentrations of the reconstituted primers were verified by recording the A^{260} of the primers using the spectrophotometer (Nanodrop). By calculating the sum of the extinction coefficients for each primer by using the primer gene sequences the following equation was used to most accurately determine the primer concentrations:

A^{260} = Sum of Extinction Coefficient x Path Length x Concentration/100

As primers are not double stranded and are considerably shorter than whole genomic DNA this method of determining concentration has greater accuracy than methods previously described. 1:10 working dilutions were made in H_2O and stored at + 4° C for future use.

The TaqMan (Applied Biosystems) probe was labeled at the 5' end with 6-carboxyfluorescein (FAM). The 3' end was labeled with TAMRA quencher. TaqMan probes allow for quantification of specific amplification products. A fluorescent signal will be detected by the RT-PCR machine only following the release of the 3' quencher by the DNA polymerase which occurs only during amplification of specific DNA sequences.

A SYBR Green (Applied Biosystems, Foster City, CA, USA) qPCR reaction was performed to test the specificity of the primers. Compared to TaqMan

probes, real-time PCR with SYBR Green yields similar data. However, SYBR Green emits a fluorescent signal upon DNA intercalation. This is less specific than TaqMan as any double stranded DNA, regardless of source, is capable of SYBR Green intercalation resulting in a false positive signal. The reaction was carried out with a final volume of 25 μL containing 12.5 μL SYBR Green Master Mix (Applied Biosystems), 0.41 μL (15.3 μM) of forward and 0.496 μL (12.6 μM) reverse primers, 5 μL template DNA, and 6.59 μL ddH_2O. The DNA template consisted of a standard curve as previously described containing GFP- positive mouse DNA. A negative control consisting of an identical standard curve created using GFP-negative mouse DNA was run. Additionally, negative controls that contained all reagents minus template DNA were run. Each SYBR Green qPCR reaction consisted of the following steps: 10 minutes at 95°C to activate the polymerase, and 40 cycles of 15 seconds denaturing at 95°C and 1 minute at 60°C of extension and annealing. Following the completion of 40 cycles a melting curve was performed to determine purity of the amplicons. Data were collected at the end of each elongation step and analyzed with iCycler iQ Real Time Detection System Software (Bio-Rad, Hercules, CA, USA). To further ensure amplicon specificity products from SYBR Green PCR were run on a 4% NuSieve 3:1 Plus Agarose Gel (Lonza Inc., Walkersville, MD, USA) in 1x TAE buffer. 8 μL of PCR product decreasing to 3 μL in 1 μL increments over successive wells were run with 2 μL loading buffer (Invitrogen, Grand Island, NY, USA). ddH_2O was used to

bring total volume to 10 μL/lane. Gel was imaged using Gel Doc XR+ System (Bio-Rad).

In an effort to ensure that the TaqMan PCR was as sensitive and specific as possible when applied to the future experiments a number of optimization experiments were performed. The optimal primer concentration was investigated by performing PCR reactions with primer concentrations of 125 nM, 250 nM, 500 nM and 1000 nM. PCR was carried out with a final volume of 20 μL containing 10 μL of TaqMan Universal PCR Master Mix-UDG (Applied Biosystems), 0.5 μL (10.0 μM) of the TaqMan probe, and 5 μL of DNA. Varying amounts of both forward and reverse primers were added as described to reach the desired concentrations and ddH_2O was added to bring the final volume of each reaction to 20 μL. The template DNA used for each reaction was the standard curve in triplicate for each primer concentration as described above. Each qPCR reaction consisted of the following steps: 2 minutes UNG incubation at 50°C to remove possible amplicon contamination, followed by 10 minutes at 95°C to activate the polymerase. 40 cycles of 15 seconds denaturing at 95°C and 1 minute at 60°C for extention and annealing were performed. Data were collected at the end of each elongation step and analyzed with iCycler iQ Real-Time PCR Detection System (Bio-Rad).

Following determination of the optimal primer concentration the experiment was repeated as described above to investigate the impact on the sensitivity and specificity of the qRT-PCR reaction that the presence of a large amount of background non-specific mouse DNA would have. The reasoning behind performing this additional experiment lay in an understanding that the vast majority of DNA present in the experimental mouse samples would be non-GFP DNA. Because of this, it was imperative to know the effects on sensitivity that this DNA could potentially play in our experiments. The qRT-PCR was performed as described previously however, $1x10^5$ genomes of GFP-negative mouse DNA was added to each reaction.

Following optimization experiments all TaqMan PCR was carried out with a final volume of 20 μL containing 10 μL of TaqMan Universal PCR Master Mix-UDG (Applied Biosystems), 0.33 μL (15.3 μM) of forward and 0.396 μL (12.6 μM) reverse primer, 0.5 μL (10.0 μM) of the TaqMan probe, up to 5 μL of DNA and 3.774 μL of ddH_2O. 6000 mouse genomes per sample were added to each reaction. For consistency, ddH_2O was added to each reaction to bring the final DNA template volume to 5 μL.

Negative controls that contained all reagents except the target DNA, along with 10-fold serial dilutions of positive control DNA were included in each

run. Additionally, explanted inferior vena cava from a GFP- negative mouse was used as a negative control.

- *Scaffold Fabrication*

The scaffolds for the TEVGs were constructed from a nonwoven polyglycolic acid (PGA) mesh (Concordia Fibers, Coventry, RI, USA) and a copolymer sealant solution of poly-L-lactide and ε-caprolactone [P(CL/LA)] using the dual cylinder chamber molding system as previously described (35).

- *BMMC isolation and TEVG assembly*

Bone marrow was collected from the femurs of syngeneic CB57BL/6 mice (Jackson Laboratories, Bar Harbor, ME, USA). Following purification of the mononuclear cell component using Histopaque-1086 (Sigma, St. Louis, MO, USA) centrifugation, 1 x 10^6 mononuclear cells were manually pipetted onto the scaffold. The seeded scaffold was incubated in Dulbecco's modified Eagle's medium (Life Technologies, North Andover, MA, USA) overnight before implantation as described previously (35).

- *TEVG Implantation*

TEVG implantations were performed using a microsurgical technique. The scaffolds were inserted into the infrarenal IVC of 6- to 8- wk-old female mice (Jackson Laboratories as previously described (35,36). All animal experiments were done in accordance with institutional guidelines for the

use and care of animals, and the Institutional Review Board at Yale University approved the experimental procedures described.

- *Transgenic Animals*

Transgenic inbred C57BL/6 mice that express green fluorescent protein (GFP) under the control of ubiquitin-C promoter were obtained (Jackson Laboratories) and bred in our laboratories. All animal procedures were approved by the Institutional Animal Care and Committee at Yale University.

- *Fate of TEVG-seeded cells*

Six- to 8-wk-old (20-25 g) C57BL/6 mice underwent implantation of IVC interposition grafts using a previously approved protocol, seeded with 1 x 10^6 GFP^+ BMMCs. Mice were killed postoperatively at 6 h (n = 4), 1 d (n = 4), 3 d (n = 4), 7 d (n = 4), and 14 d (n = 4). The grafts were explanted at predetermined time points to assess for the fate of seeded cells using quantitative realtime PCR (qRT-PCR) as described previously. Explanted grafts were placed in lysis buffer (Qiagen). DNA extraction and quantification was carried out as described above.

- *Cell Quantification Assay*

The cellularity of each GFP^+ BMMC-seeded scaffold was determined by measuring DNA content with the PicoGreen detection assay (Molecular Probes, Eugene, OR, USA). At 6 h and 1, 3, and 7 d of incubation, seeded

scaffold sections were rinsed 3 times in 1 ml PBS, placed in 200 μL of distilled water, and stored at -80°C. At the time of evaluation, scaffold sections were thawed at 37°C. A black 96-well plate was loaded with 50 μL from each sample. A 30 μL aliquot of PicoGreen dye was mixed thoroughly with 6 ml of Tris-EDTA buffer (pH 7.5), and 50 μL was added to each sample in the 96-well plate. All samples were performed in triplicate. The plate was incubated in the dark at room temperature for 10 min. Fluorescence was measured at 188 nm excitation and 525 nm emission. The number of cells maintained on each scaffold was determined from a standard curve generated from a known quantity of mouse BMMCs. A negative control of unseeded scaffold sections was used for comparison (28,37,38).

- *Cell viability assay*

To determine GFP^+ BMMC viability following seeding onto scaffold sections and incubation at 6 h and 1, 3, and 7 d, a CellTiter 96 AQ_{ueous} nonradioactive cell proliferation assay (Promega BioSciences, San Luis Obispo, CA, USA) was performed. After seeding, all scaffold sections were incubated in 2 ml of RPMI 1640 (1% penicillin/streptomycin and 10% fetal bovine serum) for the respective incubation times. Medium was changed every 2 d. Following incubation, the scaffold sections were washed 3 times with 1 ml PBS and the assay reagent, tetrazolium compound 3-(4,5-dimethylthiazol-2-yl)-5-(3-carboxymethoxyphenyl)-2-(4-sulfophenyl)-2H-tetrazolium, inner salts (MTS), and an electron coupling reagent,

phenazine methosulfate, was added to each scaffold section in a 1:4 ration with medium and allowed to incubate for 4 h at 37°C. After 4 h, a 100 μL aliquot of each sample was added to a clear 96-well plate, and the absorbance at 490 nm was read. The relative cell viability was determined by the ratio of absorbance from the seeded scaffold sections incubated at different time points.

- *Bone Marrow Transplantation*

After myeloablation with 900 cGy total body irradiation using a ^{137}Cs source, 6-wk-old female wild-type C57BL/6 mice received a tail vein injection of 5 x 10^6 unfractionated nucleated bone marrow cells (BMCs harvested from age-matched, sex-mismatched (male) GFP^+ transgenic mice, as described previously (39). We confirmed engraftment of the bone marrow 1 mo after bone marrow transplantation by determining the percentage of GFP^+ cells on peripheral blood using FACS. Subsequently, TEVGs (n = 57) were implanted as IVC interposition grafts. Specimens for immunostaining (n = 27) were explanted at postoperative d 3 (n = 6), 7 (n = 6), and 14 (n = 5), wk 10 (n = 5), and mo 6 (n = 5), and specimens for qRT-PCR (n =30) were explanted at postoperative d 3 (n = 6), 7 (n = 6), and 14 (n = 6), wk 10 (n = 6), and mo 6 (n = 6).

- *Composite Graft Construction*

The vena cava was harvested from a male mouse. Sections of the vena cava (1mm) were anastomosed to the distal end of a scaffold. The composite

scaffold was then seeded and incubated as described above. The composite TEVG was implanted in a female host (n = 8). Specimens were harvested at postoperative d 7 (n = 2) and 14 (n = 2), wk 10 (n = 2), and mo 6 (n = 2).

- *Histology*

Explanted grafts were pressure fixed in 10% formalin overnight and then embedded in paraffin or glycolmethacrylate using previously published methods (35,36). Sections were stained with hematoxylin and eosin.

- *Immunohistochemistry*

Primary antibodies included rat-anti-mouse Mac-3 (BD Bioscience, San Jose, CA, USA), F4/80 (AbD Serotec, Raleigh, NC, USA), mouse-anti-human von Willebrand Factor (vWF; Dako), rabbit-anti-mouse to c-kit (Abcam), mouse-anti-mouse to Sox-2 (R&D Systems). Antibody binding was detected using appropriate biotinylated secondary antibodies, followed by binding of streptavidin-HRP and color development with 3,3-diaminobenzidine (Vector, Burlingame, CA, USA). Nuclei were then counterstained with hematoxylin. For immunofluorescence detection, a goat=anti-rabbit IgG-Alexa Fluor 568 (Invitrogen, Carlsbad, CA, USA) or a goat-anti-mouse IgG-Alexa Fluor 488 (Invitrogen) was used with subsequent 4',6-diamidino-2-phenylindole nuclear counterstaining.

- *Fluorescent in situ hybridization* (FISH)

FISH was performed on paraffin sections using digoxigenin-labeled mouse Y chromosome probe detected using a rhodamine-conjugated antibody to digoxigenin (Roche Diagnostics, Mannheim Germany) as described previously (15, 16). Counting of Y^+ nuclei was accomplished by systematically examining the FISH-stained tissue, field by field, at x 40, using a Zeiss Axiovert 200M Fluorescence/Live cell Imaging Microscope (Carl Zeiss Imaging Solutions, Thornwood, NY, USA). Digital images were acquired using the Zeiss LSM510 confocal computer system (Carl Zeiss Imaging Solutions). Images were pseudocolored using image processing software (Adobe Photoshop, San Jose, CA, USA). Cell counts were obtained by first counting all of the Y chromosome-positive ($YChr^+$) cells in a defined area on the tissue and then counting the total number of cells in that area using the immunostained photographs.

Results:

qRT-PCR is a sensitive and specific method for the quantification of mouse DNA

The initial SYBR Green qRT-PCR experiments revealed that the sensitivity of the GFP primers was approximately 10 genomes. GFP negative mouse DNA was used in this experiment as a negative control and revealed no amplification. To ensure that detected amplification was specific for the desired region of the GFP gene a melting curve on the PCR products was performed at the conclusion of the 40^{th} PCR cycle. This revealed a consistent melting curve at 86°C at all DNA concentrations supporting that

amplification was specific (data not shown). To further investigate the specificity of the qRT-PCR reaction the PCR products were run on a 4% agarose gel to allow adequate resolution of small amplicons. A single amplification product was visualized at 98 bp which corresponded with the expected amplicon size based on the GFP sequence and primer pair used (data not shown). TaqMan qRT-PCR experiments revealed similar reaction sensitivities of 10 genomes. Primer concentrations of 1000 nM consistently resulted in increased sensitivity and thus all subsequent reactions contained a final concentration of 1000 nM for both the forward and reverse primer. The addition of 1×10^5 mouse genomes to each qRT-PCR reaction revealed no decrease in sensitivity or specificity when compared to reactions carried out without the additional mouse DNA.

TEVGs form neovessels resembling native veins

Syngeneic BMMCs seeded onto miniaturized PGA-P(CL/LA) scaffolds were subsequently implanted onto the IVC of CB57BL/6 mice. Histologic examination of explanted grafts at 6 months revealed the presence of a mature laminated structure that consisted of an endothelialized intimal layer along with a smooth muscle layer consistent with native vein tissue (Fig. 1B). Scaffold material was found to be completely degraded by 6 months. Additionally, three-dimensional computed tomography angiography of TEVGs at 6 months revealed no evidence of stenosis, aneurismal dilation, or thrombosis (Fig. 1A).

Fate of TEVG-seeded cells

qRT-PCR performed for the GFP gene present in BMMCs seeded onto the TEVG *in vitro* demonstrated that the greatest amount of GFP DNA was maximal at 6 hrs following overnight incubation (Fig. 2A). The GFP DNA present on the scaffold decreased after 1 day of incubation. These *in vitro* data suggest that seeded cells decrease in number during the initial incubation process. This is most likely secondary to a failure for the cells to adequately adhere to the scaffolding material and thus are washed off with medium changes. Cell viability and metabolic activity of the seeded BMMCs were both demonstrated to increase over a 7 day incubation period (Fig. 2B). This supports the notion that the loss of cells demonstrated over the course of incubation is due to the cells failure to adhere to the scaffolding material and not due to BMMC cell death *in vitro.*

Following 7 days of incubation TEVGs (*n=30)* that had been seeded with GFP-labeled syngeneic BMMCs were implanted onto the IVC of 6- to 8-week-old C57Bl/6 mice. The TEVGs were harvested at 6 hour, and 1, 3, 7, and 14 days. At each time point the percentage of GFP DNA was quantified. We found that the seeded GFP-labeled syngeneic BMMCs disappeared with the increase in host-derived macrophages on the scaffold. Graft immunofluorescence revealed the presence of GFP-labeled cells at 6 hours and 1 and 3 days. However, at 7 days post implantation no GFP cells were identified on the scaffold (Fig. 2C). These data were further supported by

qRT-PCR for GFP DNA on explanted TEVGs. Over the course of 14 days following graft implantation the GFP concentration on the graft was shown to decrease rapidly from a high of 173 genomes/μL at 6 hours post-implantation to 0.12 genomes/μL at 14 days post-implantation. The percentage of GFP^+ cells per TEVG was found to decrease from 4.37% at 6 hours to 0.02% at 14 days (Fig. 2E). In an effort to demonstrate that this decrease in cell percentages was due to the loss of GFP^+ cells, and not simply a result of a dilutional effect caused by the influx of host cells the data were standardized. This standardization further recapitulated that initial GFP^+ cells were indeed lost following implantation of the graft.

BMCs are not the ultimate source of vascular neotissue

Building on the aforementioned results a series of experiments were designed in an effort to identify the source of the cells that ultimately come to populate the implanted scaffold. The role of host BMCs in neotissue formation was investigated by creating chimeras of rescued lethally irradiated C57BL/6 female mice with sex-mismatched male GFP^+ total BMCs from transgenic GFP-labeled mice. Donor cell engraftment within the surviving recipients was determined at 5 weeks following bone marrow transplantation and FACS analysis of peripheral blood GFP-labeled mice demonstrated 97.74% circulating GFP+ cells in a positive control mouse (Fig. 3A), 0.49% in a negative control mouse (Fig. 3B), and 94.06% reconstitution in transplanted mice (Fig. 3C). TEVGs were implanted in female mice following successful creation of the chimeras. Following graft

implantation the mice were killed at 3, 7, and 14 days, 10 weeks, and 6 months. Grafts were evaluated histologically and YChr^{+} cells were demonstrated in the graft wall at 3 and 7 days following implantation. These cells were primarily male-derived macrophages as determined by colocalization of YChr+ and F4/80 antibody cells. These YChr^{+} BMCs continued to increase in number and at day 14 days both endothelial cells and smooth muscle cells began to appear. The cells comprising the developing neotissue were positive for vWF and SMA and negative for YChr (Fig. 4D, E). A confluent neointima comprised of endothelial cells and neomedia comprised of smooth muscle cells were present by week 10. These layers were both negative for YChr^{+} cells. Finally, the last time point at 6 months post-implantation revealed a smooth muscle layer composed of calponin+ YChr^{-} cells with a endothelial layer of vWF^{+} YChr^{-} cells (Fig. 4A, B). The original scaffold material was nearly completely degraded with the presence of scant inflammatory cells positive for MAC-3 and YChr (Fig. 5B). The infiltration of BM-derived YChr^{+} cells in the implanted graft wall increased during the initial 10 weeks following implantation, however by the 6 month time point the presence of these cells was greatly decreased (Fig. 4C). These observations provided by immunohistochemistry were further recapitulated quantitatively by using qRT-PCR for GFP DNA within the graft over an identical time course (Fig. 4D). These data revealed that following graft implantation the initial scaffold infiltrates were macrophages originating in the bone marrow. Following this initial

inflammatory infiltrate the presence of endothelial and smooth muscle cells lacking colocalization of cell markers specific to each tissue type with the Y chromosome were present with a decreasing presence of inflammatory cells (Fig. 4E).

Neovessel formation arises from ingrowth of vascular cells from the neighboring blood vessel

While the bone marrow appears responsible for an initial inflammatory infiltrate following graft implantation, the source of the endothelial and smooth muscle cells was demonstrated in previous experiments to be derived of cells not of bone-marrow-origin. An experiment was designed to investigate the possibility that the graft neotissue's origins lay in the cells of the blood vessel adjacent to the implanted graft. A composite vascular graft was created by anastomosing a segment of syngeneic male IVC with a TEVG scaffold (Fig. 5A). The entire composite vascular graft (n=8) was implanted into a female host. The grafts were harvested at 7 and 14 days, 10 weeks, and 6 months post-implantation. After paraffin embedding all grafts were cut longitudinally so that male IVC (donor), TEVG, and female (host) IVC were included. FISH specific to Y chromosome was performed on the explanted grafts. At days 7 and 14 following graft implantation the majority of the graft were populated by MAC 3^{+}/YChr^{-} cells (host origin). At these time points no confluent endothelial or smooth muscle cell layers were identified. However, at day 14 a non-confluent endothelial and smooth muscle layer positive for vWF and calponin respectively were

noted. The confluence of these cell layers was greatly increased by 10 weeks postimplantation. At 6 months postimplantation the neovessel was composed of a confluent neointima, neomedia and a neoadventitia. Using FISH it was revealed that cells comprising the neotissue adjacent to the male IVC (donor) contained the highest percentage of YChr+ cells (Fig. 5B, C). The neotissue adjacent to the female (host) IVC lacked YChr+ cells. These, along with the previously discussed findings, suggest that the cells that ultimately come to permanently populate the graft and create the viable neovessel have their origins in the vessel adjacent to the implanted scaffold. This is contrary to previous proposed mechanisms that hypothesized that the source of cells ultimately creating the neovessel were derived from the seeded cells or from bone marrow progenitor cells. Instead it suggests a mechanism involving a locally mediated process of in growth of endothelial and smooth muscle cells from the surrounding native vessel.

Discussion:

As the clinical trial performed by Shinoka has shown that the use of TEVGs in the repair of single ventricle is both effective and safe with results that clearly represent an improvement over the standard of care (29). As previously stated, despite the efficacy and excellent safety profile of TEVGs in these repairs, stenosis has continued to plague grafts requiring subsequent stenting or angioplasty to correct. With this knowledge we returned to the laboratory in an effort to elucidate the mediators of

stenosis in implanted TEVGs. This study's purpose was specifically to determine the source of the cells that ultimately create the neotissue in implanted TEVGs. In effort to make this determination, the origins of vascular neotissue cells in a syngeneic immunocompetent mouse recipient using bone marrow chimeric hosts and composite vascular implants was investigated. To mimic the high-flow, low-pressure venous setting that one would encounter in clinical applications related to the repair of congenital heart defects the PGA-P(CL/LA) tubular scaffolds were miniaturized and seeded with syngeneic BMMCs prior to implantation into the mouse IVC.

Previous work published by the laboratory was validated in the observation that the seeded cells from the TEVG following implantation disappeared precipitously. These data were of increased clinical relevance in this study in that an immune-competent murine model was used. Additionally, to track the fate of the seeded BMMCs used in this study, TEVGs that were implanted were constructed by seeding the scaffolds with GFP-labeled syngeneic BMMCs. These scaffolds were harvested over a time course of 2 weeks. At each time point the percentage of GFP-positive DNA was quantified by using RT-PCR. Findings were consistent to a previous study using a human into mouse xenogeneic model in that the seeded cells disappeared after implantation as the scaffold became populated by host-derived cells. These cells that initially populate the implanted scaffold were identified as F4/80-expression macrophages. While this decrease in the percentage of GFP-positive cells present on the TEVGs could have been

simple secondary to a dilutional effect due to the increased cell density caused by infiltrating macrophages, this possibility was ruled out by standardizing the data to reflect cell density. It was again observed, as has been described in previous studies, that over the course of 6 months following implantation the scaffold material completely degrades and the TEVGs display a vascular architecture similar to that of native vein.

The results of the previous experiments clearly show that contrary to the traditional hypothesis, the cells seeded onto the TEVG prior to implantation do not differentiate, divide and subsequently becoming the vascular neotissue observed at 6 months. Instead the source of the cells that ultimately comprise the vascular neotissue must have an alternate source. The two hypotheses that we proposed regarding the source of these cells were the host's bone marrow-derived cells or the cells comprising the adjacent vasculature itself. In an effort to address the possibility that the source of the cells were the host's bone marrow-derived cells, TEVGs were implanted into female mice that had undergone bone marrow transplantations with syngeneic male bone marrow. These TEVGs were harvested at numerous time points over the course of 6 months. Harvested grafts were analyzed using FISH for the Y chromosome. A number of other cellular markers were included as well such as F4/80 for macrophages, calponin for smooth muscle cells, and vWF for endothelial cells. These experiments revealed that the macrophages seen immediately infiltrating the TEVG following graft were positive for Y chromosome indicating that

they are derived from the bone marrow. However, at later time points after the development of vascular neotissue, there was no evidence of colocalization of either smooth muscle cell markers or endothelial cell markers with the marker for the Y chromosome. These data suggest that while the initial host response to the implanted TEVG in the form of infiltrating macrophages is derived from the host's bone marrow, the cells that ultimately become the neotissue are from an alternate source.

The second proposed hypothesis that we investigated was that the source of the cells that ultimately comprise the vascular neotissue is the neighboring blood vessel itself. A composite vascular graft created by anastomosing a segment of syngeneic male IVC proximally to the TEVG. The entire TEVG with the anastomosed male IVC was implanted into a female host. As in previous experiments these were harvested over a 6 month time period. The explanted grafts were analyzed using FISH to identify Y chromosome presence along with the presence of endothelial and smooth muscle cells. Contrary to previous experiments both endothelial cells and smooth muscle cells were found to contain the Y chromosome. Additionally, the percentage of cells that were positive for the Y chromosome was noted to be greatest adjacent to the implanted male IVC segment. As one moves distally along the implanted TEVG a decline in cells positive for the Y chromosome was noted. These data suggest that the source of cells ultimately comprising the neotissue arise from the in growth of cells from the adjacent blood vessel segments both proximally

and distally to the implanted TEVG. It is likely these cells are already fully differentiated prior to ingrowth, however our experiments cannot rule out the possibility that there exists a rare population of stem cells that reside within the adjacent vascular segments. In an effort to investigate this possibility immunohistochemistry staining was performed for both stem cells and progenitors. This staining provided no evidence for the presence of non-differentiated cells further suggesting that the source of the cells is fully differentiated neighboring endothelial and smooth muscle cells.

Our study has allowed for a significantly increased understanding of the process of TEVG formation following implantation. The most valuable information that our study provides to the understanding of the development of TEVGs is that in our mouse model the cells that become the intima and media of the neovessel are derived from the vessel wall of proximal and distal neighboring vasculature. The finding that cells seeded onto the biodegradable scaffold prior to implantation are not directly responsible for the growth of cells on the scaffold represents a paradigm shift with respect to the previous hypothesis.

The next step is to use these discoveries in the creation of a second-generation TEVG with the goal of significantly decreasing the graft stenosis rate. While grafts have been shown to remain patent following implantation without cell-seeding, the rate of stenosis and subsequent graft failure is much greater in these non-seeded TEVGs. Although our data suggest the role of seeded cells is secondary to the ultimate formation of

TEVG neotissue it is possible that they help facilitate an accelerated host response and thus expedited formation of the neovessel. This acceleration could alone account for the decrease in stenosis and graft failure due to a decrease in the amount of time that the host's pro-coagulant blood products are exposed to the scaffold material and the possible turbulent flow that may result. Future experiments should be focused on identifying critical molecular mediators of stenosis. Once these have been identified, grafts could be designed with improved long-tem patency. Secondly, the molecular mechanisms controlling vascular neotissue formation should be elucidated. Because our experiments have demonstrated that seeded cells are not directly responsible for graft population, it can be deduced that the role that the seeded cells is of paracrine nature. By identifying mediators of this paracrine response it would be possible to create grafts that elute cytokines, thus obviating the need for cell-seeding.

Preliminary studies have supported this hypothesis finding that seeded grafts recruit significantly more macrophages suggesting that this recruitment is of importance in the formation of patent neovessels. Additionally, MCP-1 along with IL-1β were detected in abundance in seeded grafts. Subsequent studies in which scaffolds containing alginate microspheres were implanted into mice revealed that the controlled release of MCP-1 allowed by the alginate microspheres prevented graft stenosis in the absence of cell seeding. These results suggest that the MCP-1 released following implantation recruit host monocytes to the graft

which participate in the formation of vascular neotissue by means of an inflammation-mediated process of vascular remodeling (40). Further studies further characterizing this process will help to further elucidate the molecular players involved with the aim of creating improved TEVGs in the future.

References:

1. LeBlanc J.G., Russell J.L. 1998. Pediatric cardiac surgery in the 1990s. *Surg Clin North Am*. 78:729-747.
2. Green A. 2004. Outcomes of congenital heart disease: a review. *Pediatr Nurs* 30:280-284.
3. Mayer J.E., Shinoka T, Shum-Tim D. 1997. Tissue engineering of cardiovascular structures. *Curr Opin Cardiol.* 12:528-532.
4. Mirensky T.L., Breuer C.K. 2008. The development of tissue-engineered grafts for reconstructive cardiothoracic surgical applications. *Pediatr Res.* 63:559-568.
5. Samanek M. 1992. Children with congenital heart disease: probability of natural survival. *Pediatr Cardiol.* 1992. 13(3):152-158.
6. Fontan F., Baudet E. 1971. Surgical repair of tricuspid atresia. *Thorax.* 26:240-248.
7. Giannico S., Hammad F., Amodeo A., Michielon G., Drago F., et al. 2006. Clinical outcome of 193 extracardiac Fontan patients: the first 15 years. *J Am Coll Cardiol.* 47(10):2065-2073.
8. Petrossian E., Reddy V.M., Collins K.K., Culbertson C.B., MacDonald M.J., et al. 2006. The extracardiac conduit Fontan operation using minimal approach extracorporeal circulation: early and midterm outcomes. *J Torac Cardiovasc Surg.* 132(5):1054-1063.
9. De Leval M.R., Kilner T., Gewillig M., Bull C. 1988. Total cavopulmonary connection: a logical alternative to atriopulmonary connection for complex Fontan operations. Experimental studies and early clinical experience. *J Thorac Cardiovasc Surg.* 96:682-695.
10. Forbess J.M. 2004. Conduit selection for right ventricule outflow tract reconstruction: contemporary options and outcomes. *Semin Thorac Cardiovasc Surg Pediatric Card Surg Annu.* 7:115-124.
11. Tokunaga S., Kado H., Imoto Y., Masuda M., Shiokawa Y., et al. 2002. Total cavopulmonary connection with an extracardiac conduit: experience with 100 patients. *Ann Thorac Surg.* 73:76-80.
12. Hufnagel C.A., Harvey W.P. 1953. The surgical correction of aortic regurgitation preliminary report. *Bull Georgetown Univ Med Cent.* 6:60-61.
13. Jonas R. Commentary on: Petrossian E., Reddy V.M., McElhinney D.B., Akkersdiuk G.P., Moore P., et al. 1999. *J Thorac Cardiovasc Surg.* 117:688-696.

14. Dearani J.A., Danielson G.K., Puga F.J., Schaff H.V., Warnes C.W., et al. 2003. Late follow-up of 1095 patients undergoing operation for complex congenital heart disease utilizaing pulmonary ventricle to pulmonary artery conduits. *Ann Thorac Surg.* 75(2):399-410.
15. Albert J.D., Bishop D.A., Fullerton D.A., Campbell D.N., Clarke D.R. 1993. Conduit reconstruction of the right ventricular outflow tract: lessons learned in a twelve-year experience. *J Thorac Cardiovasc Surg.* 106:228-236.
16. Kay P.H., Ross D.N. 1985. Fifteen years' experience with the aortic homograft: the conduit of choice for right ventricular outflow tract reconstruction. *Ann Thorac Surg.* 40:360-364.

17. Alexi-Meskishvili V., Ovroutski S., Ewert P., Dahnert I., Berger F., Lange P.E., Hetzer R. 2000. Optimal conduit size for extracardiac Fontan operation. *Eur J Cardiothorac Surg.* 18(6):690-695.
18. Petrossian E., Reddy V.M. McElhinney D.B., Akkersdijk G.P., Moore P., et al. 1999. Early results of the extracardiac conduit Fontan operation. *J Thorac Cardiovasc Surg.* 117(4):688-696.
19. Shinoka T., Shum-Tim D., Ma P.X., Tanel R.E., Isogai N., et al. 1998. Creation of viable pulmonary artery autografts through tissue engineering. *J Thorac Cardiovasc Surg.* 115(3):536-545.
20. Matsumura G., Hibino N., Ikada Y., Kurosawa H., Shin'oka T. 2003. Successful application of tissue engineered vascular autografts: clinical experience. *Biomaterials.* 24(13):2303-2308.
21. Matsumura G., Ishihara Y., Miyagawa-Tomita S., Ikada Y., Matsuda S., et al. 2006. Evaluation of tissue-engineered vascular autografts. *Tissue Eng.* 12(11):3075-3083.
22. Watanabe M., Shin'oka T., Tohyama S., Hibino N., Konuma T., et al. 2001. Tissue-engineered vascular autograft: inferior vena cava replacement in a dog model. *Tissue Eng.* 7(4):429-439.
23. McAllister T.N., Maruszewski M., Garrido S.A., Wystrychowski W., Dusserre N. et al. 2009. Effectiveness of haemodialysis access with an autologous tissue-engineered vascular graft: a multicentre cohort study. *Lancet.* 272(9673):1440-1446.
24. Hoenicka M., Lehle K., Jacobs V.R., Schmid F.X., Birnbaum D.E. 2007. Properties of the human umbilical vein as a living scaffold for a tissue-engineered vessel graft. *Tissue Eng*. 13(1):219-229.
25. Daly C.D., Campbell G.R., Walker P.J., Campbell J.H. 2004. In vivo engineering of blood vessels. *Front Biosci.* 9:1915-1924.
26. Hibino N., McGillicuddy E., Matsumura G., Ichihara Y., Naito Y., Breuer C., Shinoka T. 2010. Late-term results of tissue-engineered vascular grafts in humans. *J Thorac Cardiovasc Surg.* 139(2):431-436, 436 e431-432.
27. Naito Y.,Imai Y., Shin'oka T., Kashiwagi J., Aoki M., et al. 2003. Successful clinical application of tissue-engineered graft for extracardiac Fontan operation. *J Thorac Cardiovasc Surg.* 125(2):419-420.
28. Shin'oka T., Imai Y., Ikada Y. 2001. Transplantation of a tissue-engineered pulmonary artery. *N Engl J Med*. 344(7):532-533.

29. Shin'oka T., Matsumura G., Hibino N., Naito Y., Watanabe M., et al. 2005. Midterm clinical result of tissue-engineered vascular autografts seeded with autologous bone marrow cells. *J Thorac Cardiovasc Surg.* 129:1330-1338.
30. Isomatsu Y., Shinoka T., Matsumura G., Hibino N., Konuma T., et al. 2003. Extracardiac total cavopulmonary connection using a tissue-engineered graft. *J Thorac Cardiovasc Surg.* 126:1958-1962.
31. Langer, R., and Vacanti J.P. 1993. Tissue Engineering. *Science.* 260, 920-926.
32. Gragerov, A., Horie K., Pavlova M., Madisen L., Zeng H. 2007. Large-scale, saturating insertional mutagenesis of the mouse genome. *Proc Natl Acad Sci USA.* 104(36):14406-11.
33. Shimomura O., Johnson F., Saiga Y. 1962.Extraction, purification and properties of aequorin, a bioluminescent protein from the luminous hydromedusan, Aequorea. *J Cell Comp Physiol.* 59(3):223-39.
34. Thastrup O., Tulin S., Kongsbak Poulsen L., Bjorn S. 2001. Fluorescent Proteins. *US patent.*
35. Roh J.D., Nelson G.N., Brennan M.P., Mirensky T.L., Yi T., et al. 2008. Small-diameter biodegradable scaffolds for functional vascular tissue engineering in the mouse model. *Biomaterials.* 29,1434-1463.
36. Roh J.D., Sawh-Martinez R., Brennan M.P., Jay S.M., Devine L., et al. 2010. Tissue-engineered vascular grafts transform into mature blood vessels via an inflammation-mediated process of vascular remodeling. *Proc Natl. Acad.* 107, 4669-4674.
37. Roh J.D., Nelson, G.N., Udelsman, B. V., Brennan, M.P., Lockhart, B., et al. 2007. Centrifugal seeding increases seeding efficiency and cellular distribution of bone marrow stromal cells in porous biodegradable scaffolds. *Tissue Eng.* 13, 2743-2749.
38. Villalona, G.A., Udelsman, B., Duncan, D.R., McGillicuddy, E., Sawh-Martinez, R.F., et. al. Cell-seeding techniques in vascular tissue engineering. *Tissue Eng. B Rev.* 16, 341-350.
39. Di Lorenzo A., Fernandez-Hernando C., Cirino G., and Sessa W.C. 2009. Akt1 is critical for acute inflammation and histamine-mediated vascular leakage. *Proc Natl Acad Sci.* 106, 14552-14557.
40. Roh J.D., Sawh-Martinez R., Brennan M.P., Jay S.M., Devine L., et al. 2010. Tissue-engineered vascular grafts transform into mature blood vessels via an inflammation-mediated process of vascular remodeling. *Proc Natl Acad Sci USA.* 107(10):4669-46754.

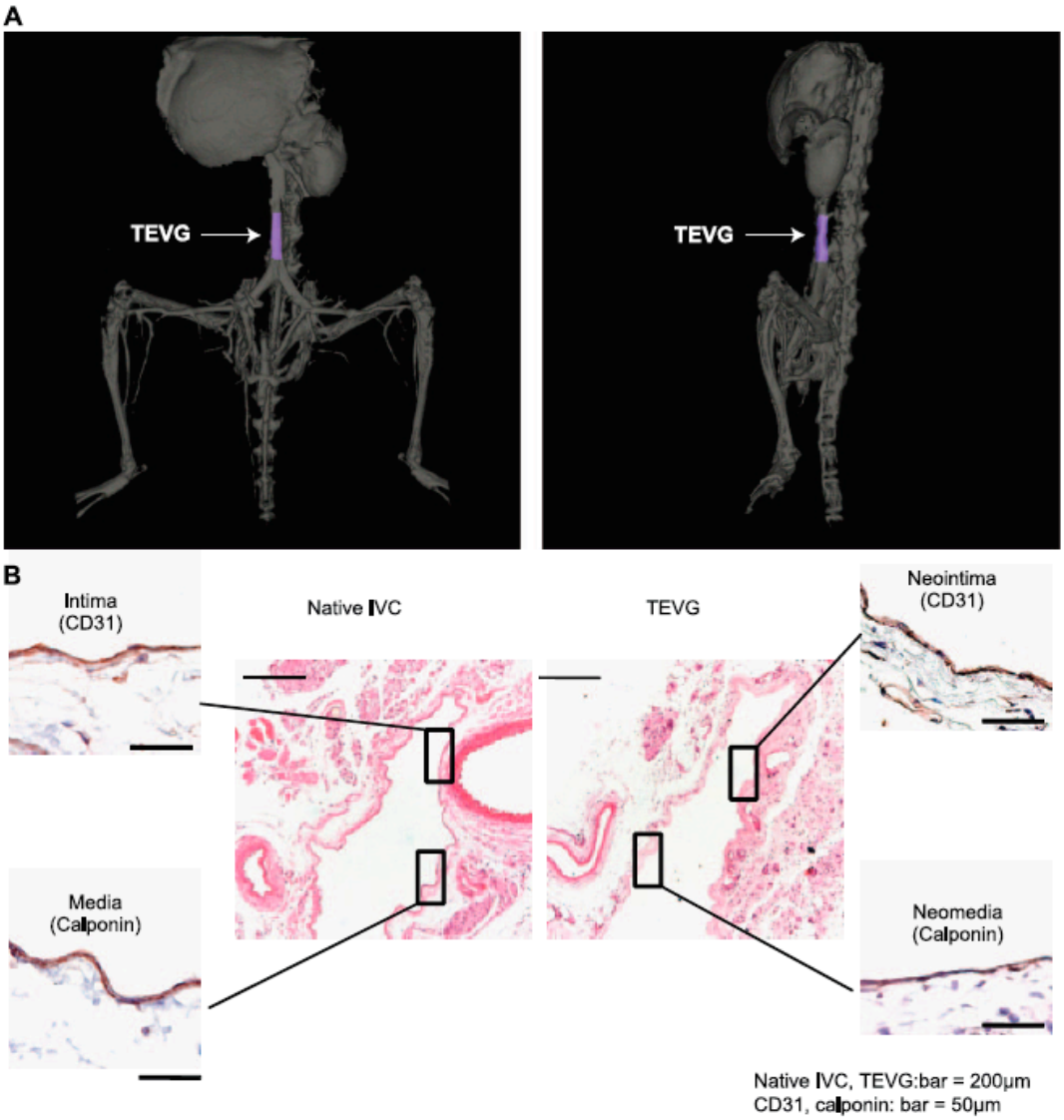

Figure 1. A) CT angiogram of a TEVG IVC interposition graft 6 mo after implantation. TEVG is colored blue. B) Representative photomicrographs of immunohistochemical characterization of the native IVC compared with the TEVG 6 mo after implantation (hematoxylin and eosin, x100; CD31 and Cal, x400).

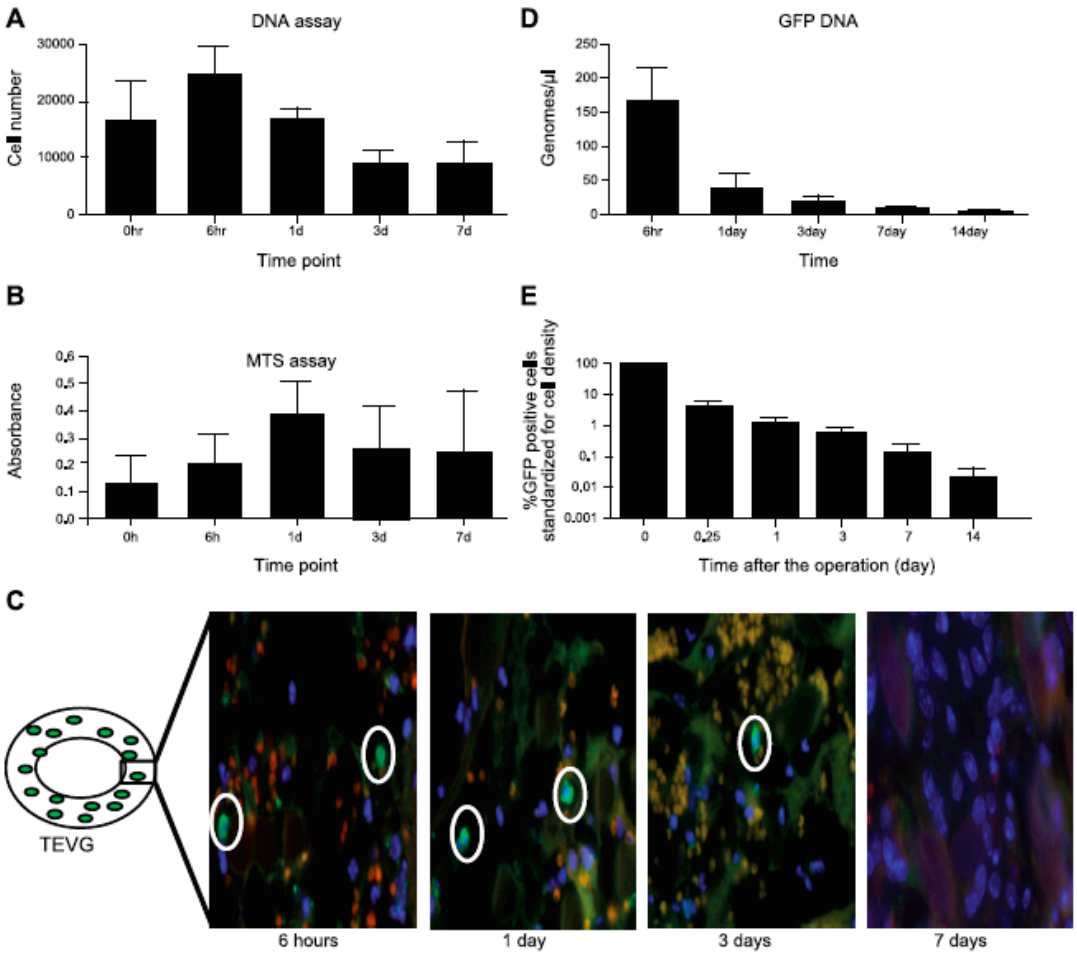

Figure 2. A) DNA assay of scaffolds from 0 h to 7 d of *in vitro* incubation showed increased number of cells in first 24 h and loss of cells after 72 h. B) MTS assay of scaffolds from 0 h to 7 d *in vitro* incubation showed initial increase in metabolic activity followed by steady state. C) *In vivo* tracking using immunofluorescence (x630) demonstrated GFP⁺ cells within the graft at 6 h and 1 and 3 d but no cells at 7 d postimplantation. D) These findings were corroborated by qRT-PCR for the GFP gene from TEVGs (n=30) seeded with GFP⁺ cells, implanted in GFP-negative hosts, and harvested between 6 h and 14 d after implantation. Level of detection is 10 genomes/µl. E) Percentage of GFP-labeled cells per TEVG standardized for cell density decreased form 4.37% at 6 h to 0.02% at 14 d. Data are expressed as means ± SD.

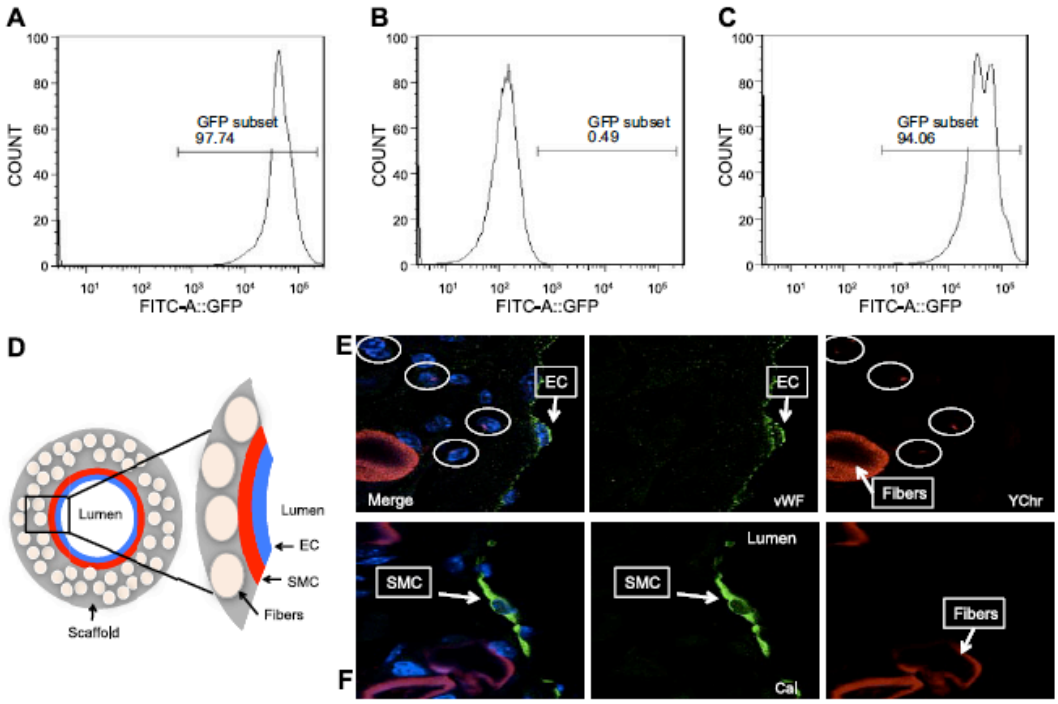

Figure 3. A-C) FACS analysis of GFP$^+$ mouse as positive control (A), C57BL/6 mouse for negative control (B), and engraftment 5 wk post-transplantation (C). D) Schematic demonstrating components and orientation of photomicrographs. E, F) Confocal microscopic images of TEVG implanted into female host that had undergone transplantation with male bone marrow harvested 14 d after implantation, demonstrating no colocalization with the Y chromosome (Y-chromosome FISH and either endothelial cells (EC; vWF, x630; E) or smooth muscle cells (SMC; calponin, x630; F).

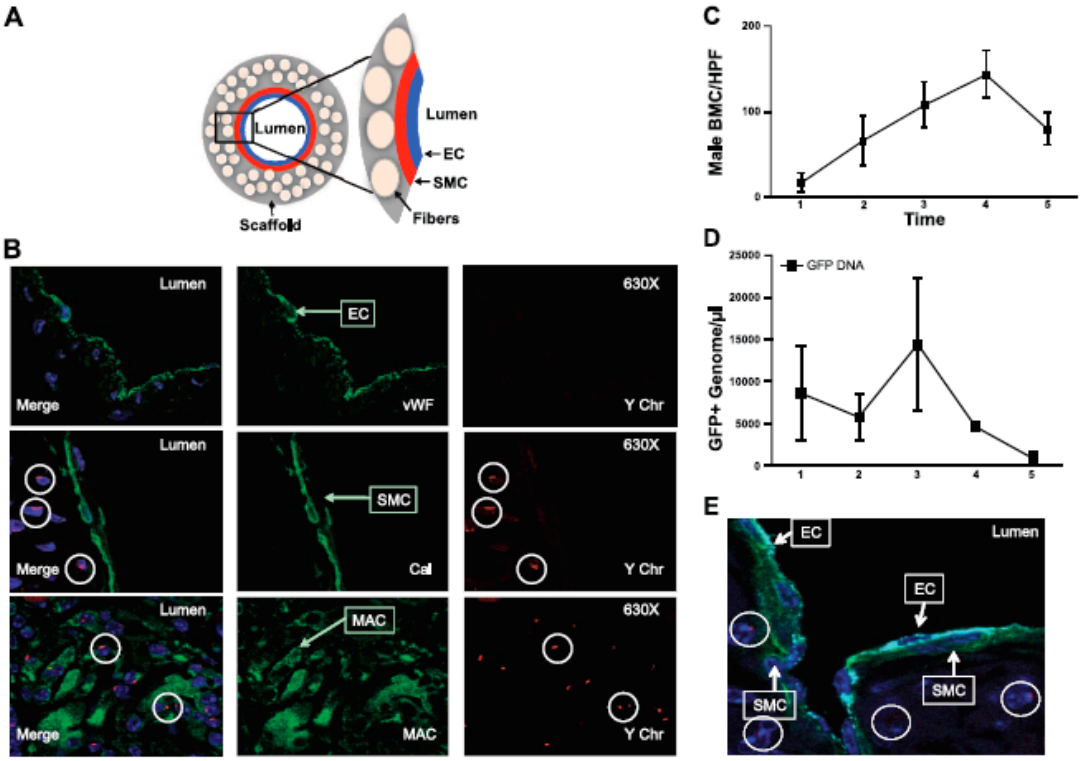

Figure 4. A)Schematic demonstrating components and orientation of photomicrographs. B) Confocal microscopic images of TEVG implanted into female host that had undergone transplantation with male bone marrow harvested 6 mo after implantation, demonstrating colocalization of macrophages (MAC) and the Y-chromosome (Y-chromosome FISH) but no colocalization with the Y chromosome (Y-chromosome FISH) and either endothelial cells (vWF) or smooth muscle cells (Calponin; x400). C) Numbers of infiltrating BM-derived Y chromosome (Y-chromosome FISH) cells (bone marrow cells/high power field) in the graft wall increased up to 10 wk, while graft degradation was occurring, but at 6 mo postimplantation, these cells markedly decreased. D) This was quantified and corroborated using qRT-PCR for GFP DNA within the graft over a 6 mo period. E) Confocal microscopic image of triple staining of a 6 mo neovessel with normal IVC configuration with single-layer neointima (EC;vWF/light blue), neomedia (SMC; calponin/green), and neoadventitia with scattered inflammatory cells (male;Ychr/red).

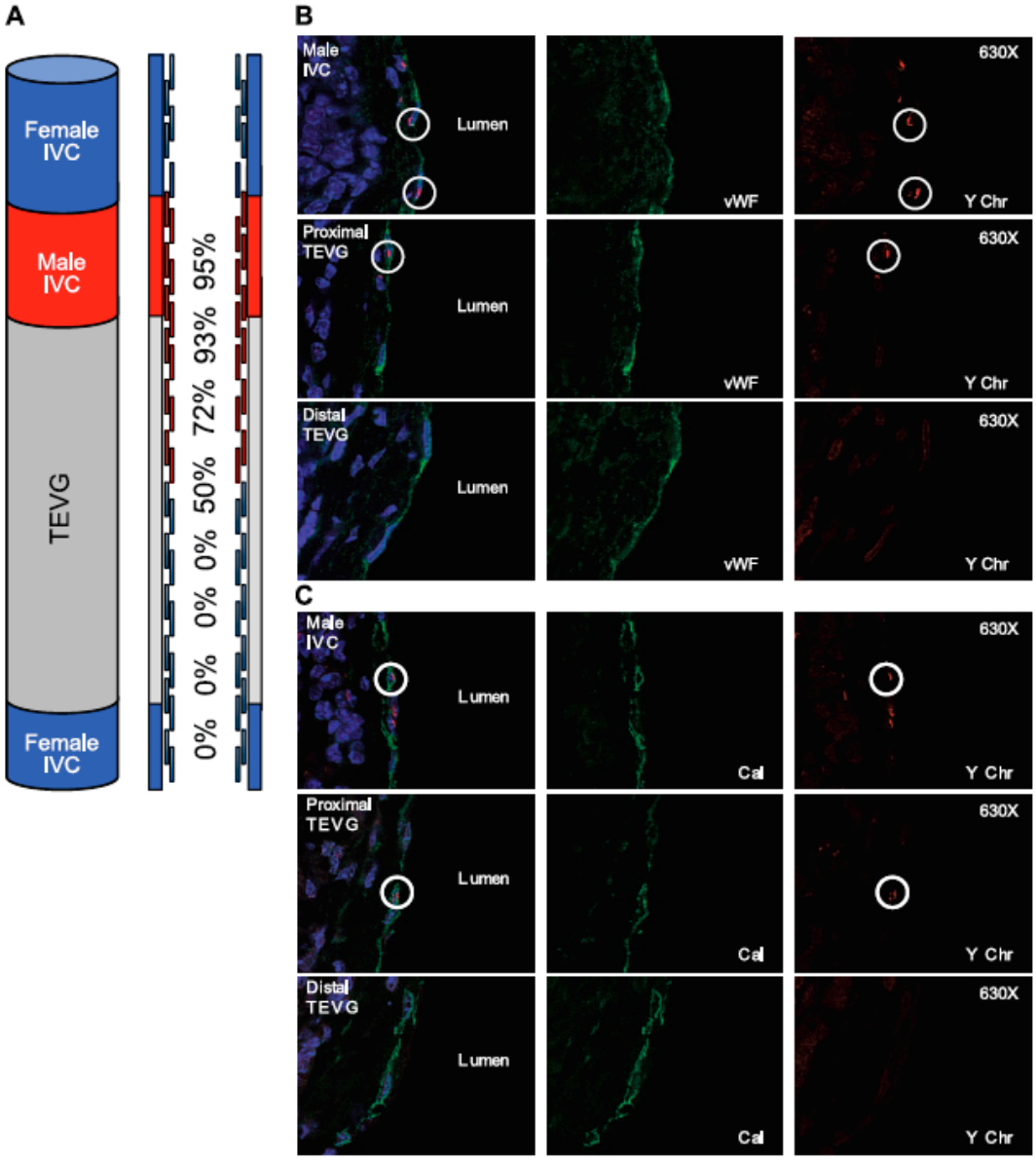

Figure 5. Schematic demonstrating composite TEVG (*n*=8) created by anastomosis of a syngeneic male IVC with a TEVG, implanted into a female host and harvested at 6 mo after implantation, and the percentage of cells with Y-chromosome as a function of distance from the male IVC. A) Confocal microscopic images demonstrating colocalization of endothelial cells (VWF) and Y chromosome (Y chromosome FISH;x400). C) Photomicrographs demonstrating colocalization of smooth muscle cells (calponin) and Y chromosome (Y-chromosome FISH; x400).